

Images/LogoUPC.eps

PROGRAMA DE DOCTORAT EN ENGINYERIA BIOMÈDICA  
DEPARTAMENT D'ENGINYERIA DE SISTEMES,  
AUTOMÀTICA I INFORMÀTICA INDUSTRIAL  
CENTRE DE RECERCA EN ENGINYERIA BIOMÈDICA

Tesis Doctoral por compendio de publicaciones

**Muscular pattern based on multichannel surface EMG  
during voluntary contractions of the upper-limb**

Mislav Jordanic

September 2017

Directores:

Miguel Angel Mañanas Villanueva  
Mónica Rojas-Martínez



# Abstract

Magnetoencephalography (MEG) is a noninvasive brain signal acquisition technique that provides excellent temporal resolution and a whole-head coverage allowing the spatial mapping of sources. These characteristics make MEG an appropriate technique to localize the epileptogenic zone (EZ) in the preoperative evaluation of refractory epilepsy.

Presurgical evaluation with MEG can guide the placement of intracranial EEG (iEEG), the current gold standard in the clinical practice, and even supply sufficient information for a surgical intervention without invasive recordings, reducing invasiveness, discomfort, and cost of the presurgical epilepsy diagnosis. However, MEG signals have low signal-to-noise ratio compared with iEEG and can sometimes be affected by noise that masks or distorts the brain activity. This may prevent the detection of interictal epileptiform discharges (IEDs) and high-frequency oscillations (HFOs), two important biomarkers used in the preoperative evaluation of epilepsy.

In this thesis, the reduction of two kinds of interference is aimed to improve the signal-to-noise ratio of MEG signals: metallic artifacts mask the activity of IEDs; and the high-frequency noise, that masks HFO activity. Considering the large number of MEG channels and the long duration of the recordings, reducing noise and marking events manually is a time-consuming task. The algorithms presented in this thesis provide automatic solutions aimed at the reduction of interferences and the detection of HFOs.

Firstly, a novel automatic BSS-based algorithm to reduce metallic interference is presented and validated using simulated and real MEG signals. Three methods are tested: AMUSE, a second-order BSS technique; and INFOMAX and FastICA, based on high-order statistics. The automatic detection algorithm exploits the known characteristics of metallic-related interferences. Results indicate that AMUSE performs better when recovering brain activity and allows an effective removal of artifactual components.

Secondly, the influence of metallic artifact filtering using the developed algorithm is evaluated in the source localization of IEDs in patients with refractory focal epilepsy. A comparison between the resulting positions of equivalent current dipoles (ECDs) produced by IEDs is performed: without removing metallic interference, rejecting only channels with large metallic artifacts, and after BSS-based reduction. The results show that a significant reduction on dispersion is achieved using the BSS-based reduction procedure, yielding feasible locations of ECDs in contrast to the other approaches.

Finally, an algorithm for the automatic detection of epileptic ripples in MEG using beamformer-based virtual sensors is developed. The automatic detection of ripples is performed using a two-stage approach. In the first step, beamforming is applied to the whole head to determine a region of interest. In the second step, the automatic detection of ripples is performed using the time-frequency characteristics of these oscillations. The performance of the algorithm is evaluated using simultaneous intracranial EEG recordings as gold standard.

The novel approaches developed in this thesis allow an improved noninvasive detection and localization of interictal epileptic biomarkers, which can help in the delimitation of the epileptogenic zone and guide the placement of intracranial electrodes, or even to determine these areas without additional invasive recordings. As a consequence of this improved detection, and given that interictal biomarkers are much more frequent and easy to record than ictal episodes, the presurgical evaluation process can be more comfortable for the patient and in a more economic way.

# Resumen

La magnetoencefalografía (MEG) es una técnica no invasiva de adquisición de señales cerebrales que proporciona una excelente resolución temporal y una cobertura total de la cabeza, permitiendo el mapeo espacial de las fuentes cerebrales. Estas características hacen del MEG una técnica apropiada para localizar la zona epileptogénica (EZ) en la evaluación preoperatoria de la epilepsia refractaria.

La evaluación quirúrgica con MEG puede orientar la colocación del EEG intracranegal (iEEG), el actual modelo de referencia en la práctica clínica, e incluso suministrar información suficiente para una intervención quirúrgica sin registros invasivos; reduciendo la invasividad, la incomodidad y el costo del diagnóstico de la epilepsia quirúrgica. Sin embargo, las señales MEG tienen baja relación señal ruido en comparación con el iEEG pudiendo imposibilitar la detección de descargas epileptiformes interictales (IEDs) y oscilaciones de alta frecuencia (HFOs), dos importantes biomarcadores utilizados en la evaluación preoperatoria de la epilepsia.

En esta tesis, la reducción de dos tipos de interferencia está dirigida a mejorar la relación señal-ruido de la señal MEG: los artefactos metálicos que enmascaran la actividad de las IEDs; y el ruido de alta frecuencia, que enmascara la actividad de las HFOs. Debido al gran número de canales MEG y la larga duración de los registros, tanto reducir el ruido como seleccionar los biomarcadores manualmente es una tarea que consume mucho tiempo. Los algoritmos presentados en esta tesis aportan soluciones automáticas dirigidas a la reducción de interferencias y la detección de HFOs.

En primer lugar, se presenta y valida un nuevo algoritmo automático basado en BSS para reducir interferencias metálicas mediante señales simuladas y reales. Se prueban tres métodos: AMUSE, una técnica BSS de segundo orden; y INFOMAX y FastICA, basados en estadísticos de orden superior. El algoritmo de detección automática utiliza las características conocidas de la señal producida por la interferencia metálica. Los resultados indican que AMUSE recupera mejor la actividad cerebral y permite una eliminación efectiva de componentes artefactuales.

Posteriormente, se evalúa la influencia del filtrado de artefactos metálicos en la localización de IEDs en pacientes con epilepsia focal refractaria. Se realiza una comparación entre las posiciones resultantes de dipolos de corriente equivalentes (ECDs) producidos por IEDs: sin eliminar interferencias metálicas, rechazando solamente canales con elevados artefactos metálicos y, por último, después de una reducción utilizando el algoritmo BSS desarrollado. Los resultados

muestran que se logra una reducción significativa en la dispersión utilizando el procedimiento de reducción basado en BSS, lo que produce ubicaciones factibles de los dipolos en contraste con los otros enfoques.

En segundo lugar, se desarrolla un algoritmo para la detección automática ripples epilépticos en MEG utilizando sensores virtuales basados en la técnica de beamformer. La detección de ripples se realiza mediante un enfoque en dos etapas. Primero, se determina el área de interés usando beamformer. Posteriormente, se realiza la detección automática de ripples utilizando las características en tiempo-frecuencia. El rendimiento del algoritmo se evalúa utilizando registros iEEG simultáneos.

Los nuevos enfoques desarrollados en esta tesis permiten una detección no invasiva mejor de los biomarcadores interictales, que pueden ayudar a delimitar la zona epileptogénica y guiar la colocación de electrodos intracraneales, o incluso determinar estas áreas sin este tipo de registros. Como consecuencia de esta mejora en la detección, y dado que los biomarcadores interictales son mucho más frecuentes y fáciles de registrar que los episodios ictales, la evaluación quirúrgica puede ser más cómoda y menos costosa para el paciente.

# Contents

<b>Abstract</b>	i
<b>Resumen</b>	iii
<b>List of Tables</b>	vii
<b>List of Figures</b>	ix
<b>1 Spatial distribution of HD-EMG in task identification</b>	1
1.1 Background . . . . .	2
1.2 Materials and Methods . . . . .	5
1.2.1 Simulated data . . . . .	5
1.2.2 Blind source separation approaches to artifact reduction . . . . .	8
1.2.3 Performance assessment . . . . .	11
1.3 Results . . . . .	12
1.3.1 Simulated data . . . . .	12
1.3.2 Blind source separation and automatic detection . . . . .	12
1.3.3 Performance assessment . . . . .	14

1.3.4	Real data . . . . .	16
1.4	Discussion . . . . .	18
1.5	Acknowledgments . . . . .	21

# List of Tables

1.1 Error percentage for nMSE, delta power and alpha power (average of all channels) for non-corrected signals, AMUSE-corrected signals and INFOMAX-corrected signals. . . . .	16
--	----



# List of Figures

1.3	Sum of the linear regression coefficients normalized with respect to its maximum for all of the selected artifactual patterns for the 10 simulated MEG sets. Coefficients were obtained for the whole head after morphology selection and linear regression of each channel with the selected morphologies. Note that metallic artifacts behave differently depending on their nature and therefore they can appear in different areas of the head for each simulated MEG set. . . . .	13
1.4	MEG channels (16 distributed evenly on the scalp) for: (a) control subject, that is, clean recording, free of metallic artifacts; (b) simulated subject. Orange traces indicate channels originally selected as artifacts by the experts. . . . .	14
1.5	Artifact-reduction for a simulated subject: (a), (b) and (c) show the first 20 extracted ICs corresponding to AMUSE, INFOMAX and FastICA algorithms, respectively. Note that the first 2 ICs (orange traces) obtained by AMUSE and INFOMAX were automatically selected and removed to perform signal reconstruction, whose results are shown in (d) and (e), respectively. FastICA was not able to extract useful artifact-related components and the reconstruction shown in (f) does not remove any amount of artifact (and, consequently, the reconstructed signals equal those of figure 1.4(b)). . . . .	15
1.6	Error percentage for normalized MSE, delta power and alpha power, shown for three different simulated subjects as examples. Errors are shown for non-corrected, AMUSE-corrected and INFOMAX-corrected signals. Due to the frequency content of metallic artifacts, errors are expected to be lower in the alpha band and higher in the delta band, focusing especially on the areas where the artifact is located. Note that AMUSE-based reconstruction shows the lowest errors for the three measures. . . . .	16
1.7	(a) Five-second epoch of raw MEG signals containing prominent metallic interference. Posterior channels are shown as an example. (b) Corrected MEG signals obtained after applying automatic AMUSE-based metallic removal procedure. . .	17

1.8 (a) Topographic distribution of the average alpha power of the 10 artifactual subjects. (b) Average of alpha power obtained after applying automatic AMUSE-based metallic removal procedure. . . . .	18
--	----



## Chapter 1

# Spatial distribution of HD-EMG improves identification of task and force in patients with incomplete spinal cord injury

**Published as:** Jordanić, M., Roja-Martínez, Mañas, M.A., Alonso J.F. Spatial distribution of HD-EMG improves identification of task and force in patients with incomplete spinal cord injury *Journal of NeuroEngineering and Rehabilitation* 13(1):41, 2016

doi: 10.1186/s12984-016-0151-8

Impact Factor: 3.222; Position: 3 of 65 (Q1) REHABILITATION, 12 of 77 (Q1) BIOMEDICAL ENGINEERING.

**Abstract:** *Background.* Recent studies show that spatial distribution of High Density surface EMG maps (HD-EMG) improves the identification of tasks and their corresponding contraction levels. However, in patients with incomplete spinal cord injury (iSCI), some nerves that control muscles are damaged, leaving some muscle parts without an innervation. Therefore, HD-EMG maps in patients with iSCI are affected by the injury and they can be different for every patient. The objective of this study is to investigate the spatial distribution of intensity in HD-EMG

recordings to distinguish co-activation patterns for different tasks and effort levels in patients with iSCI. These patterns are evaluated to be used for extraction of motion intention. *Method.* HD-EMG was recorded in patients during four isometric tasks of the forearm at three different effort levels. A linear discriminant classifier based on intensity and spatial features of HD-EMG maps of five upper-limb muscles was used to identify the attempted tasks. Task and force identification were evaluated for each patient individually, and the reliability of the identification was tested with respect to muscle fatigue and time interval between training and identification.

*Results.* Three feature sets were analyzed in the identification: 1) intensity of the HD-EMG map, 2) intensity and center of gravity of HD-EMG maps and 3) intensity of a single differential EMG channel (gold standard). Results show that the combination of intensity and spatial features in classification identifies tasks and effort levels properly ( $\text{Acc} = 98.8\%$ ;  $S = 92.5\%$ ;  $P = 93.2\%$ ;  $SP = 99.4\%$ ) and outperforms significantly the other two feature sets ( $p < 0.05$ ).

*Conclusion.* In spite of the limited motor functionality, a specific co-activation pattern for each patient exists for both intensity, and spatial distribution of myoelectric activity. The spatial distribution is less sensitive than intensity to myoelectric changes that occur due to fatigue, and other time-dependent influences.

**Keywords:** Myoelectric control, Pattern recognition, High-density electromyography, Incomplete spinal cord injury

## 1.1 Background

change this run-  
Magnetoencephalography (MEG) is a noninvasive and functional neuroimaging technique used in clinical practice that measures magnetic fields generated by synchronous brain oscillations. MEG has become an important tool in neurological signal processing and functional neuroimaging (??). During the last decade, an increasing number of studies of language and cognitive functions and brain connectivity have been carried out (??). Modern multichannel whole head systems such as MEG are increasingly being used for clinical applications such as the presurgical evaluation of children and adults requiring invasive surgery as a result of refractory epilepsy or brain tumors (?). This evaluation involves mainly the detection of the spatial focus that should be removed through source localization techniques (?). Several studies claim that MEG adds

valuable information to the source localization that is not visible with other imaging techniques such as electroencephalography (EEG) or functional Magnetic Resonance Imaging (fMRI) (???).

The magnetic activity of the brain is substantially smaller (starting from a few tenths of femtoteslas) than ambient noise and this is the main reason why MEG recordings are performed in a magnetically shielded room to isolate them from external magnetic fields. However, as with EEG recordings, some artifacts are unavoidable because subjects may be affected by ocular, cardiac, muscular and other interferences (?) that have to be removed or reduced using signal processing techniques before proper analysis of MEG signals can be performed. In this context, Blind Source Separation (BSS) is one of the most commonly used techniques to achieve an effective removal of several kinds of artifacts.

A drawback of MEG is its increased sensitivity to metallic interference that may come from inside the head, such as implanted intracranial electrodes and dental ferromagnetic prosthesis and brackets, or from outside, such as pacemakers and vagal stimulators (?). To try to minimize the effect of these interferences, an extremely magnetic hygiene inside the shielded room is required (?). Recordings have to be performed with subjects trying to avoid any kind of movement, and even a demagnetization of the subject can be carried out. For this reason, MEG signal recording requires very careful preparation that can only be performed by highly trained specialists. Despite all precautions, sometimes it is not possible to eliminate all sources of metallic artifacts and highly distorted recordings are obtained. Typically, these artifacts appear modulated by breathing and cardiac rhythms (?) due to the great sensitivity to movement. The amplitude of metallic artifacts is typically much higher than the amplitude of cerebral signals and can even reach values larger than  $10^5$  fT (?). Metallic artifacts affect the whole record, overlapping brain activity, and may alter all head channels with varying amplitudes. Usually, there are a certain number of channels whose high level of contamination masks cerebral activity almost completely.

The most widely used method for extracting useful information from contaminated recordings is to remove artifactual channels and to apply band-pass filtering, but there are still a large number of cases with unusable signals due to huge artifact contamination. This results in a loss of information that is particularly necessary when artifacts overlap the cerebral region of interest, for example during preparation of surgery. The literature reports few techniques able

to eliminate this sort of metallic interference. For sources located outside the head, temporal Signal Space Separation (tSSS) has been used for metallic artifact reduction using generated metallic signals in a phantom experiment (?). To do so, it was necessary to previously identify source patterns at the cost of potentially removing true brain signals as well (?).

BSS techniques have proven effective for automatically removing cardiac, ocular and movement artifacts (??) but, to date, there have not been any studies that use BSS to remove metallic artifacts in an automatic fashion. The goal of BSS algorithms is to estimate the different original source signals or components from the observation signals assuming a linear mixture model. This can be done because, although original source signals and the mixing system are unknown, a certain statistical independence between sources is assumed.

The main aim of this study was to develop an automatic algorithm based on BSS techniques to effectively remove metallic artifacts from MEG signals. It was necessary to evaluate objectively and quantitatively the performance of different BSS methods. Consequently, three well-known algorithms were evaluated: AMUSE, a second order method; and INFOMAX and FastICA, both high order statistics. Semi-automatic AMUSE-based filtering was previously evaluated on a very preliminary study with four real MEG signals (?) and its main conclusion stated that AMUSE was able to extract components projecting on the areas where metallic artifacts had more energy. However, the objective evaluation of the effectiveness of each artifact reduction process is difficult to assess with real signals because the components belonging either to artifacts or to brain signals are not fully known. To date, BSS has been tested in EEG simulated signals to reduce artifacts from external sources such as ocular interference (??), but it has not been evaluated using simulated MEG data. Therefore, simulated MEG recordings corresponding to clean signals contaminated with real metallic artifacts were generated in this study to evaluate the effectiveness of separation into components and the subsequent artifact reduction. Previous knowledge of the behavior of metallic artifacts was useful to develop a fully automatic method for the selection of source components related to artifacts, which should be subsequently removed to obtain a successful reconstruction of MEG data.

## 1.2 Materials and Methods

### Subjects and instrumentation

Ten subjects with ferromagnetic implants (age  $23.6 \pm 10.4$  years), six of them with an implanted subdural grid and four with dental brackets, and ten subjects without implants or other metallic artifactual sources (age  $36.7 \pm 10.7$  years) were selected for this study. MEG signals were acquired during 10 min with closed eyes using a whole-head 148-channel magnetometer system (4D-Neuroimaging/BTi) and sampled at 678.19 Hz (bandwidth DC to 250 Hz). Signals were imported into MATLAB using the Fieldtrip toolbox (?), and two-minute epochs were selected randomly.

Implant-related artifacts contaminated a large number of channels, some of them with a very high amplitude that masked the cerebral activity completely, which could not be extracted using classical filtering techniques. Artifacts were observed to follow regular or periodic patterns that were present with varying intensity to many channels.

#### 1.2.1 Simulated data

In order to simulate real cases of MEG signals affected by metallic interference, a linear mixture between clean signals and metallic artifacts extracted from contaminated signals was proposed, following a scheme analogous to that proposed in (?) for the generation of simulated signals affected by ocular artifacts. Ten two-minute epochs were simulated according to the following mixing model:

$$S = C + WP \quad (1.1)$$

where  $S$  indicates the simulated signals,  $C$  denotes clean MEG recordings,  $W$  corresponds to the mixture weights, and  $P$  represents the different artifactual morphologies selected. These different patterns caused by metallic interference had to be extracted from contaminated recordings and then added to clean signals according to the propagation coefficients obtained by means of an approach based on linear regression.

**Extraction of different metallic artifactual waveforms from contaminated recordings**

Most noticeable metallic artifacts are easily identifiable on visual inspection of the signals mainly due to their higher amplitude with respect to the remaining MEG channels, but also to their slower and more regular waveforms, which are usually modulated by the heart or respiratory rates (?). In this study, three experts examined the signals and identified channels that clearly and strictly met these criteria of high amplitude, low frequency, regularity, and possible modulation by respiratory or cardiac rhythms. Only those channels selected by all three experts were chosen as artifactual channels and therefore used to obtain the artifactual waveforms. The interobserver agreement was of  $0.829 \pm 0.097$  with a kappa index of  $0.851 \pm 0.095$ , indicating an 'almost perfect' agreement according to the definitions given in (?).

In order to extract only the information provided by metallic interference, a low-pass filter with the cutoff frequencies obtained with the cumulative spectra was applied to remove the cerebral activity present in these selected channels ( $7.4 \pm 2.1$  Hz as mean and standard deviation for all channels). The spectra of clean and artifactual signals were similar at high frequencies but they differed at low frequencies due to metallic interference. Considering that this conspicuous difference was due to the presence of the metallic artifact, reverse-cumulative (from high to low frequency) spectra were obtained for each artifactual channel and for the same channel in all artifact-free recordings. Spectra were calculated by means of Welch's periodogram using a five-second Hanning window with 50% overlapping. The difference between the artifactual spectrum and the average of all clean spectra was used to obtain the cutoff frequency for each artifactual channel, searching for the frequency where the normalized difference reached 5% (see figures 1.1(a) and (b)). Subsequently, each selected artifactual channel was filtered with an 8th-order Butterworth filter (figure 1.1(b)).

Metallic interference is known to affect different MEG channels with varying shape and intensity. For this purpose, a selection of the different waveforms spreading over the scalp had to be performed. Consequently, the cross-correlation between artifactual channels was obtained, and only low-correlated waveforms (coefficient  $< 0.5$ ) were preserved. Among those showing high correlation ( $\geq 0.5$ ), only the signal with the highest energy was maintained (see figure 1.1(c)). In this way, only those morphologies that were different enough were selected as artifactual

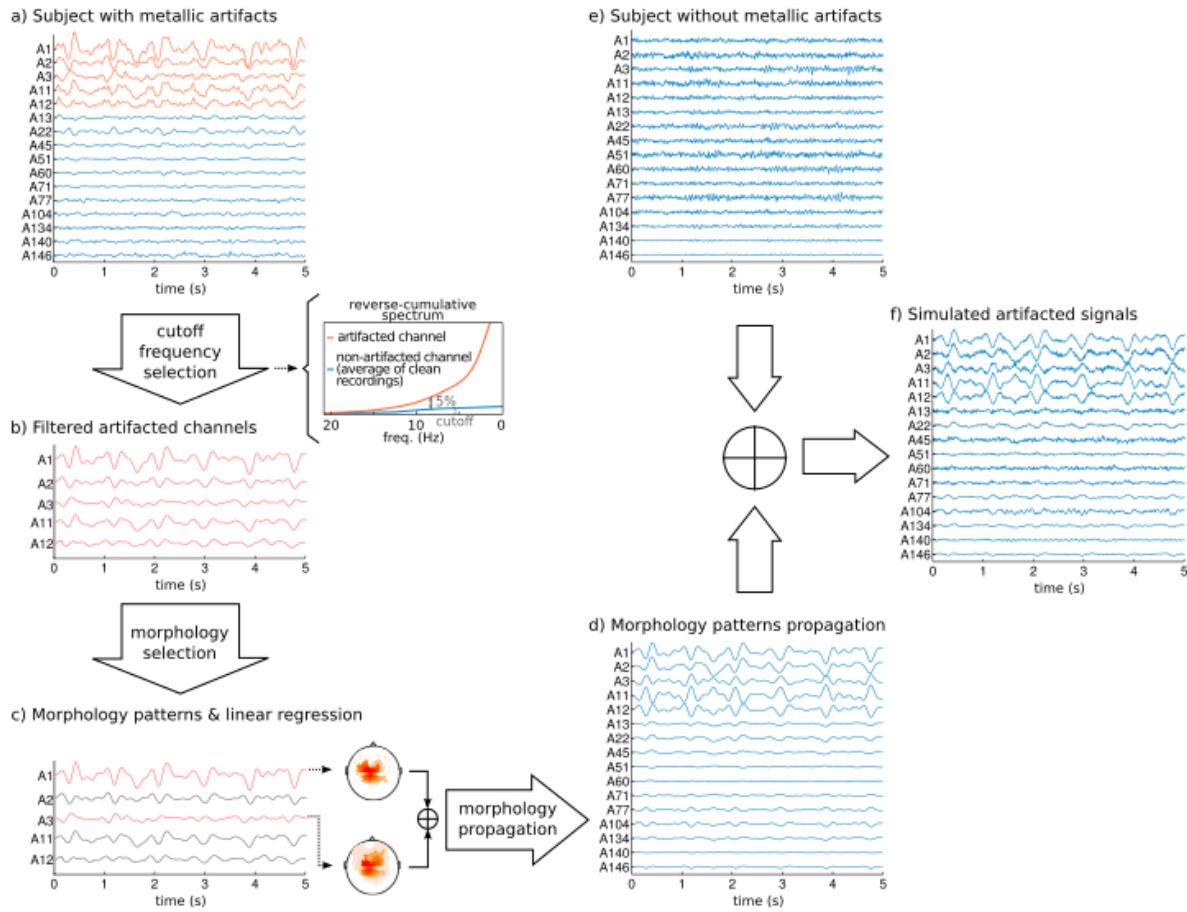


Figure 1.1: Scheme for generation of a simulated artifactual MEG recording: (a) five-second epoch of raw MEG with metallic artifacts (only 16 selected channels are drawn). Orange traces correspond to the highly artifactual channels selected by the experts; (b) low-pass filtered artifactual channels (cutoff frequency automatically calculated from reverse-cumulative spectra); (c) selected morphologies (orange traces) after correlation among channels in (b), and their corresponding linear regression coefficients (whole head maps); (d) propagation of artifacts corresponding to coefficients obtained in (c); (e) five-second epochs of raw artifact-free MEG channels; and (f) simulated signals obtained by summation of (d) and (e).

patterns (figure 1.1(d)).

### Calculation of propagation coefficients by linear regression and generation of simulated data

Propagation coefficients represented the amount of metallic interference that was present in a particular MEG channel with respect to a specific artifactual pattern. Linear regression between all channels of the actual artifactual recordings and each selected pattern was performed, taking into account the entire two-minute recordings. The obtained regression coefficients (represented

as topographic maps in figure 1.1 (c)) were used as weights of the mixing matrix  $\mathbf{W}$  (equation 1.1) and then patterns were propagated to all channels (figure 1.1(d)). Finally, the simulated artifacts were added to clean recordings (figure 1.1(e)) to obtain a set of simulated artifactual signals (figure 1.1(f)). These steps were performed 10 times to obtain 10 sets of simulated MEG signals with known metallic interference.

### 1.2.2 Blind source separation approaches to artifact reduction

BSS techniques estimate source signals from a set of mixed signals, separating MEG signals into spatial components to later reconstruct the brain signal discarding the components associated with artifacts. The model of the identification process is expressed by:

$$x(t) = As(t) \quad (1.2)$$

where  $x(t)$  is the observation signal vector and  $s(t)$  the unknown source signal vector with  $n$  and  $m$  rows respectively.  $A$  is the  $n \times m$  mixing matrix which should be estimated and represents the weights of the projection of the corresponding source signals at different channels.

Usually, BSS methods can be classified according to the order of the statistic used to perform the separation. Methods based on second order statistics (SOS) assume sources that are only uncorrelated. One of the techniques used in this study is the Algorithm for Multiple Unknown Signals Extraction (AMUSE) (?), which exploits SOS through a first step of signal whitening and a second step of an eigenvalue decomposition. AMUSE is sometimes classified as an independent component analysis (ICA) technique because decorrelation can be considered as a weak form of statistical independence (?). However, SOS are effectively enough to separate and remove those Independent Components (IC) corresponding to various types of artifacts (?).

While SOS-based algorithms provide independence in terms of correlation, in the case of higher order statistics (HOS) a more general concept is considered: two random variables are independent when the statistical behavior of one of them is not affected by the values taken by the other. Statistical independence can be estimated using several different methods based on mutual information, non-gaussianity or maximum likelihood, for example. Additionally to AMUSE, two

HOS-based techniques, INFOMAX and FastICA, were used in this work. Both algorithms are iterative and require proper initialization and parameter setting.

On the one hand, INFOMAX maximizes the joint entropy of a neural processor output, based on the fact that the maximum entropy of joint variables only occurs when they are statistically independent (?). In this study, separation by means of an extended version of INFOMAX was performed using the default parameters proposed in the EEGLAB toolbox for MATLAB (??)

On the other hand, FastICA is based on a fixed-point iterative scheme that maximizes non-gaussianity as a measure of statistical independence between sources. A weight matrix is obtained after a certain number of iterations, but non-gaussianity of the independent components is necessary for a successful convergence of the algorithm (?). However, the step size can be adjusted through a stabilization parameter so that convergence can be achieved in unfavorable conditions.

Automatic selection of metallic-related components For all three algorithms evaluated, a decomposition scheme that provided as many ICs as available MEG channels was used (148). Once the components were estimated, it was necessary to design an automatic selection procedure to detect those components related to metallic artifacts, taking into account their known features: low frequency and regular behavior, especially modulated by the heart and breathing rhythms. Two criteria were considered to identify the extracted independent components related to metallic artifacts (figure 1.2(a)):

- (i) The frequency below which the spectrum holds most of the energy of the signal. If the spectral content is located principally at low frequencies, it is more likely that the component corresponds to metallic interference.
- (ii) The regularity of the signal, as measured by the sample entropy (?). This criterion was directly associated with the typical modulation of metallic artifacts, which makes them more regular than cerebral activity.

The procedure carried out in order to select the artifactual components was based on two steps: the selection of the artifactual region and a comparison of this region with the projection of each IC.

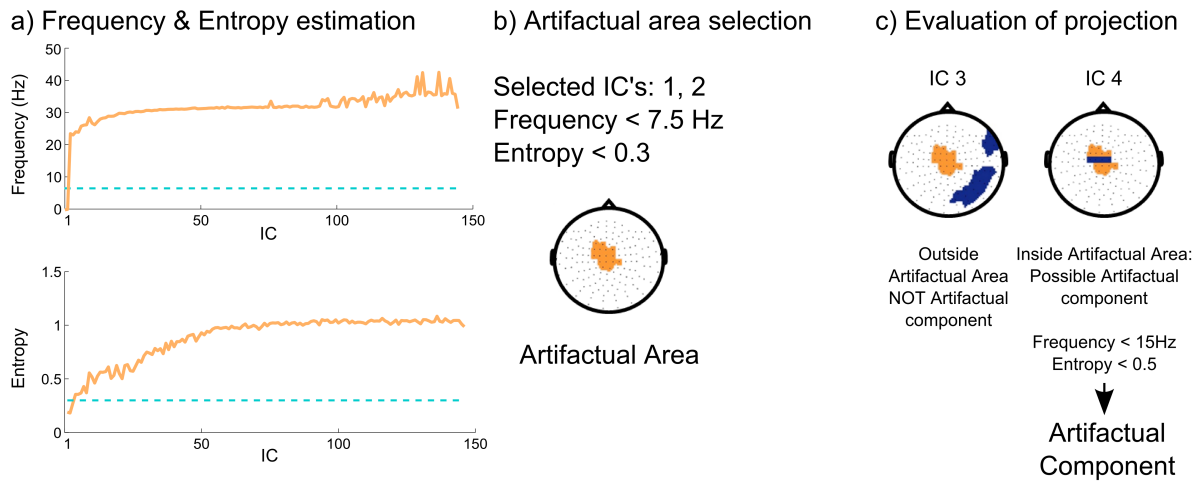


Figure 1.2: Automatic artifact-related component selection: (a) frequency and entropy estimation (for all extracted ICs) and thresholds (blue dashed lines). (b) Artifactual area selected by the union of the regions of interest of the selected ICs. (c) As an example, evaluation of the projection of ICs 3 and 4 is shown. Regions of interest are indicated with dark blue shading. IC 3 is outside the artifactual area and therefore would not be selected by the automatic algorithm, whereas IC 4 would, as its region of interest is inside the artifactual area and the weak criteria concerning frequency and entropy are met.

The purpose of the first step was to locate the artifactual area that, due to the particular origin of metallic artifacts, could be located anywhere on the scalp. In this first step, those components which simultaneously met the two above-mentioned criteria were selected as artifactual components (figure 1.2(b)) and used to identify the area of the scalp where the artifact was located. A strong version of the criteria was applied, and only ICs with 90% of the energy in the slowest frequency bands delta and theta (up to 7.5 Hz) and high regularity (sample entropy lower than 0.3, obtained with an embedding dimension of 3 and a search radius of 0.1 times the standard deviation of the signal) were selected.

A region of interest was defined for each selected component, taking into account the BSS weights normalized with respect to the maximum for each channel and discarding the lowest quartile. The final artifactual region was defined as the union of the regions of each component. The purpose of this selection was to define a region where the artifact projected and to prevent artifactual regions being focused on only a few high-energy channels.

The second step involved the comparison between the artifactual region and the region of interest of every IC (figure 1.2(c)). When this region of interest was included in the artifactual region and an IC fulfilled a weak version of the aforementioned criteria (90% of energy below 15 Hz, sample

entropy lower than 0.5), then the IC under evaluation was marked as an artifactual component. This second step was performed in order to ensure the selection of artifactual components that displayed characteristics highly related to metallic interference and were focused on the defined artifactual region. To achieve an effective removal of metallic interference, all marked ICs had to be removed, and the resulting artifact-free signal was obtained as the product of the remaining components by the weight matrix obtained by the algorithm.

### 1.2.3 Performance assessment

In order to assess the performance of the metallic artifact removal methodology, several error measurements based on time and frequency domain were calculated for each channel and each simulated recording.

- (i) The normalized mean squared error (nMSE),

$$NMSE_n = 100 \cdot \frac{\sum_i^N (x_n(i) - y_n(i))^2}{\sum_i^N y_n(i)^2} \quad (1.3)$$

- (ii) The variation of absolute power in the delta band (0.5 to 4 Hz) was obtained to study the error in the band most affected by metallic artifacts.

$$\Delta\delta = 100 \cdot \frac{\delta_x - \delta_y}{\delta_y} \quad (1.4)$$

where  $\delta_x$  and  $\delta_y$  represent the power of the  $\delta$  band of the filtered MEG channel under evaluation and of the original clean signal respectively.

- (iii) The variation of absolute power in the alpha band (7.5 to 13 Hz) was also calculated in order to observe the error made in a band where metallic artifacts should have little influence, and therefore errors should be lower.

$$\Delta\alpha = 100 \cdot \frac{\alpha_x - \alpha_y}{\alpha_y} \quad (1.5)$$

where  $\alpha_x$  and  $\alpha_y$  represent the power in the  $\alpha$  band of the signal under evaluation and of the original clean signal respectively.

## 1.3 Results

### 1.3.1 Simulated data

Ten simulated datasets were generated following the steps explained in figure 1.1. The number of channels containing visible metallic interference selected by the experts was  $6.6 \pm 4.4$ , and, in general, artifacts contaminated channels with varying amplitudes. While in some subjects the high amplitude of the artifacts affected many channels, there were other cases where high amplitudes focused on a reduced number of channels. In spite of the dispersion shown by the location of the artifact, their associated signals showed low frequency and regular pattern characteristics, modulated by cardiac and respiratory rates.

Once the different waveforms (patterns) were obtained, and after proper filtering and correlation procedures explained in the previous sections, propagation to the whole head was performed by means of linear regression. Figure 1.3 shows the propagation coefficients normalized with respect to the maximum obtained after regression. It is noticeable that metallic artifacts affected different areas of the scalp depending on the subject, and while in some cases artifacts were focused at specific regions, in others they appeared more dispersed and covered a larger area of the head.

### 1.3.2 Blind source separation and automatic detection

Separation of ICs was performed with AMUSE, INFOMAX and FastICA for the ten simulated subjects. AMUSE and INFOMAX algorithms successfully extracted ICs from the mixed signals in which artifact-related source components were visually identifiable. Subgaussianity of the data, especially related to metallic artifacts, caused a non-effective decomposition in the case of the FastICA algorithm, which could not separate ICs related to brain signals from metallic artifacts even after using the stabilization parameters to ensure convergence.

The automatic detection procedure was applied to the obtained ICs to detect which components were associated with the metallic interference and therefore were to be discarded to obtain a successful removal of metallic artifacts.

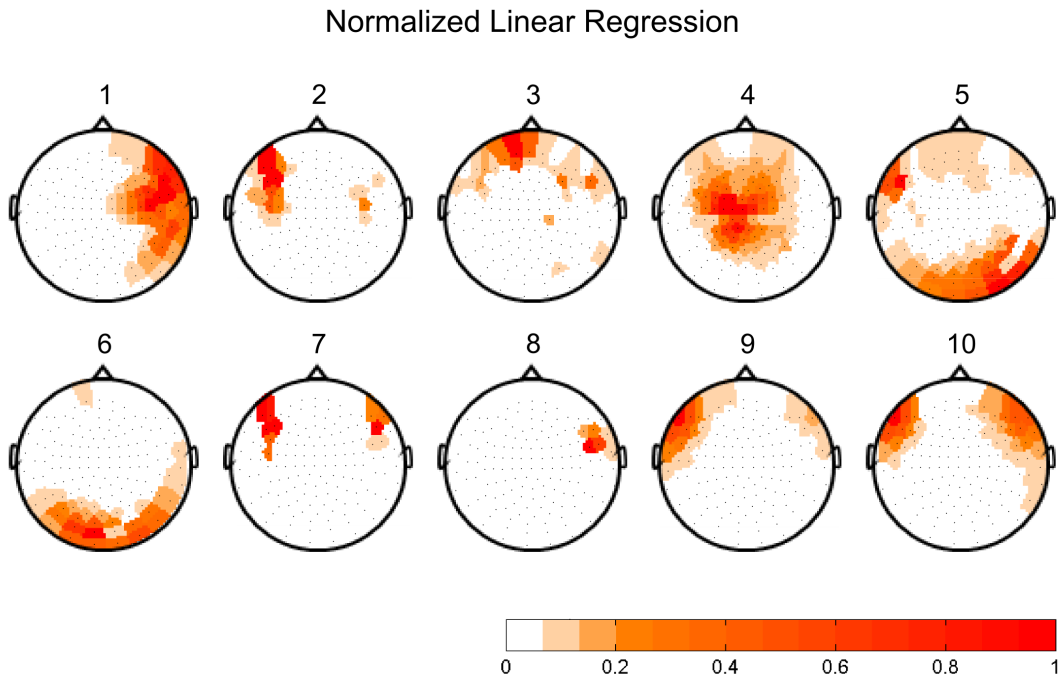


Figure 1.3: Sum of the linear regression coefficients normalized with respect to its maximum for all of the selected artifactual patterns for the 10 simulated MEG sets. Coefficients were obtained for the whole head after morphology selection and linear regression of each channel with the selected morphologies. Note that metallic artifacts behave differently depending on their nature and therefore they can appear in different areas of the head for each simulated MEG set.

Figure 1.4(a) shows, as an example, an artifact-free subject signal; and figure 1.4(b) shows the simulated signals obtained after the addition of artifactual waveforms to the same subject. Figure 1.5 shows the results, in time domain, of the artifact reduction process on simulated signals shown in figure 1.4. Figures 1.5(a), (b) and (c) show the extracted ICs for AMUSE, INFOMAX and FastICA respectively, with the selected ICs displayed in a different color. The resulting signals obtained after reconstruction without considering the ICs associated with metallic interference are shown in figures 1.5(d), (e) and (f). It is noticeable that the automatic algorithm procedure was not able to identify any metallic-related ICs in the FastICA decomposition, and this led to a full reconstruction of the signal with the original metallic interference. Visual inspection of the extracted components and the reconstructed signals indicated that INFOMAX was not completely successful in separating brain-related activity from artifactual waveforms, but AMUSE was indeed able to separate metallic interference from MEG activity. INFOMAX provided components related to artifactual activity mixed with cerebral waveforms and the effects of such a decomposition were remarkable after signal reconstruction (figure 1.5(e)), especially

when compared to AMUSE (figure 1.5(d)), which showed much more similar signals compared to the clean set (figure 1.4(a)).

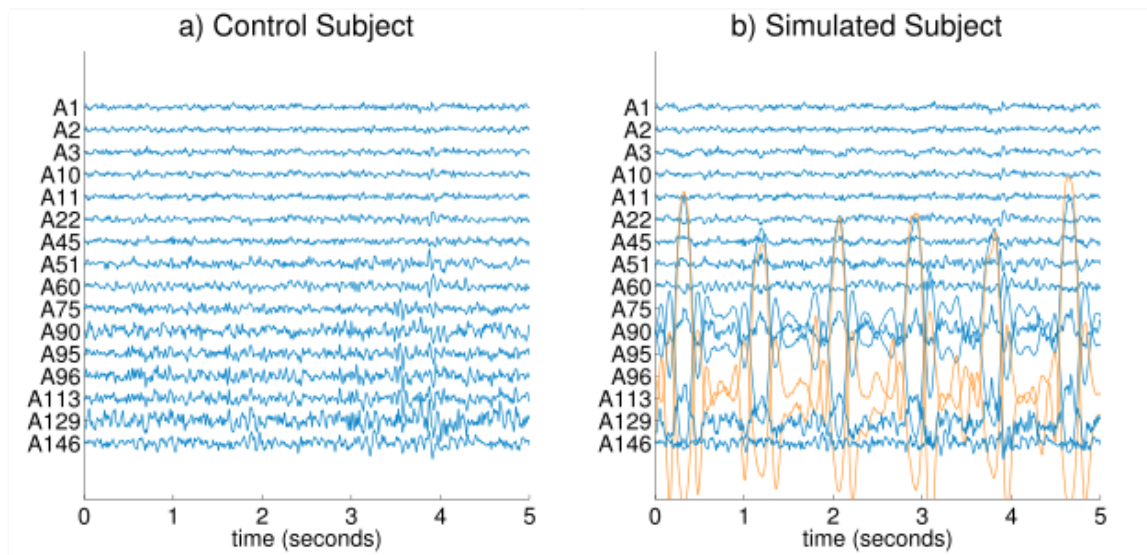


Figure 1.4: MEG channels (16 distributed evenly on the scalp) for: (a) control subject, that is, clean recording, free of metallic artifacts; (b) simulated subject. Orange traces indicate channels originally selected as artifacts by the experts.

### 1.3.3 Performance assessment

Figure 1.6 shows the percentage error in several subjects as an example, represented as whole-head topographic maps. These errors were calculated for three conditions: simulated signals without correction, to observe the amount of artifact introduced; and after applying AMUSE- and INFOMAX-based artifact filtering. Metallic contamination was mainly present in the area of high-energy artifacts, while the distortion of the remaining channels was considerably lower. For this reason the amount of error observed for the uncorrected case always showed a maximum error value in the artifactual region. As expected, errors in the delta frequency band after filtering were higher than in the alpha band because of the characteristics of metallic contamination, and INFOMAX showed higher errors than AMUSE.

As explained in the previous sections, metallic contamination masked the cerebral activity of some channels in real cases. This situation was reproduced in the simulated MEG subjects and, in fact, the energy introduced by metallic artifacts in MEG activity was huge in many cases

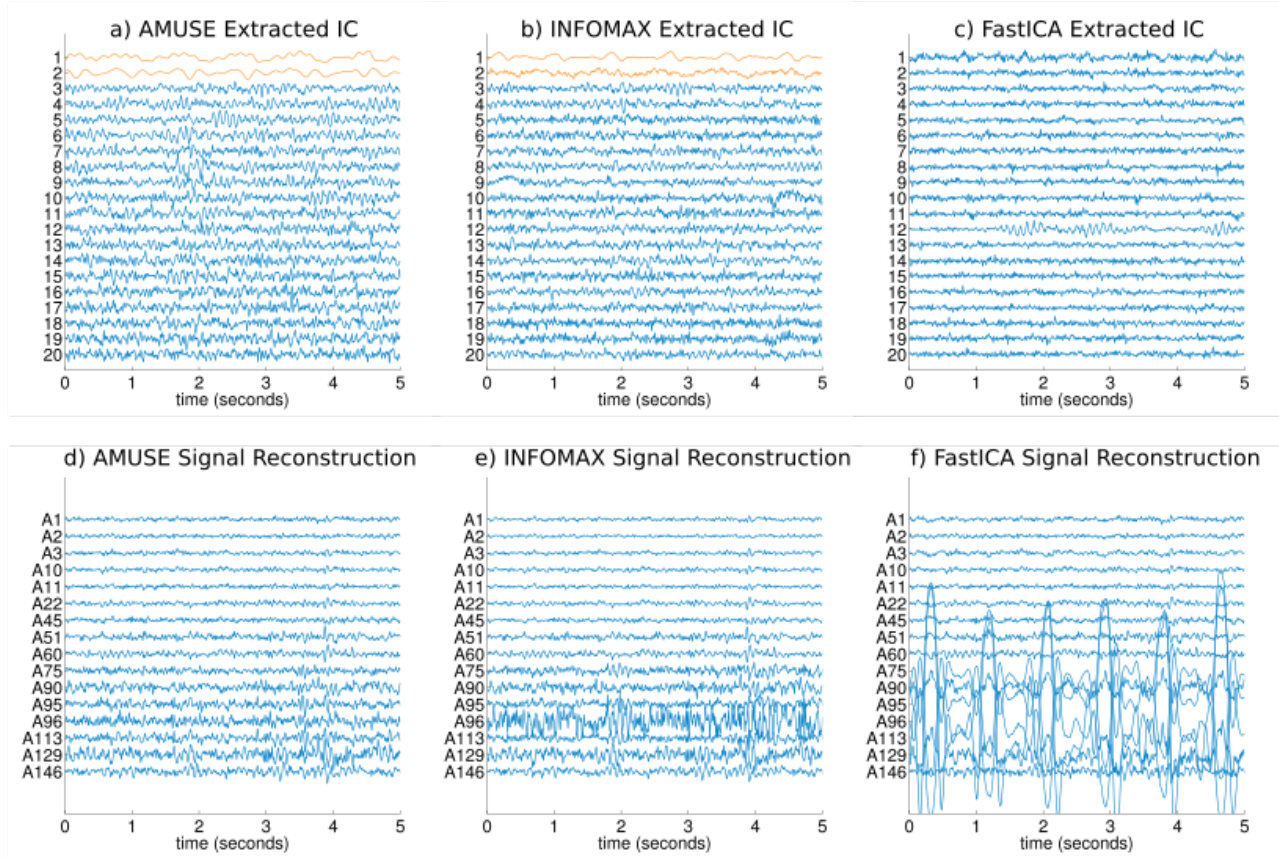


Figure 1.5: Artifact-reduction for a simulated subject: (a), (b) and (c) show the first 20 extracted ICs corresponding to AMUSE, INFOMAX and FastICA algorithms, respectively. Note that the first 2 ICs (orange traces) obtained by AMUSE and INFOMAX were automatically selected and removed to perform signal reconstruction, whose results are shown in (d) and (e), respectively. FastICA was not able to extract useful artifact-related components and the reconstruction shown in (f) does not remove any amount of artifact (and, consequently, the reconstructed signals equal those of figure 1.4(b)).

(see values and average in table 1.1). After applying INFOMAX-based correction, this error was reduced but still high, whereas after AMUSE-based filtering this error was lower than 1%.

The variability in amplitude and energy of metallic artifacts caused the amount of error introduced to be very inhomogeneous. As can be observed in figure 1.6, INFOMAX was not an appropriate method to remove the interference because of the large amount of error obtained: the error provided in the alpha band, sometimes higher than without correction, suggested that INFOMAX ICs associated with artifacts were a mixture of metallic and cerebral signals, and possibly some brain-related activity was being deleted. On the contrary, AMUSE always provided low alpha power errors, below 3%.

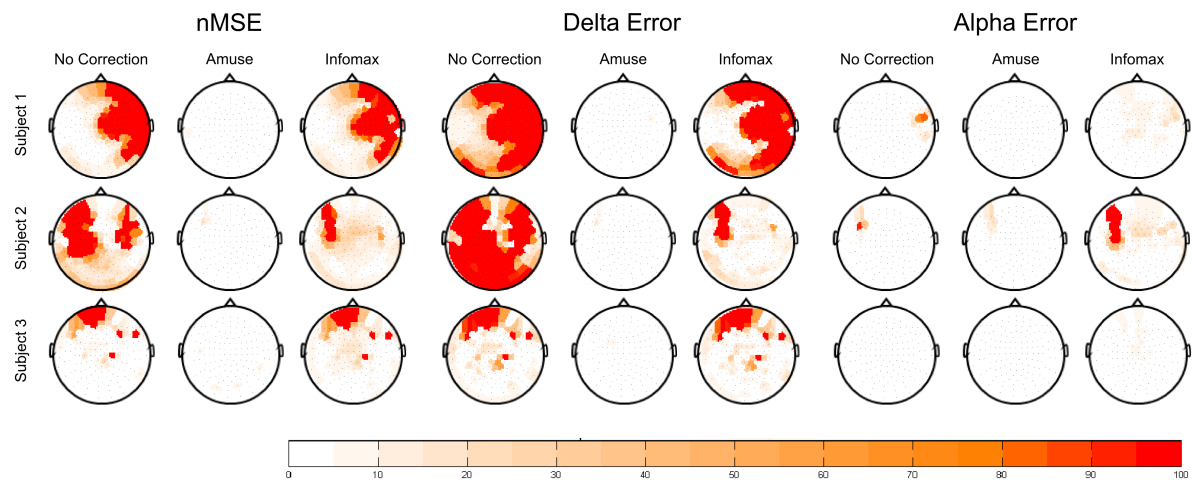


Figure 1.6: Error percentage for normalized MSE, delta power and alpha power, shown for three different simulated subjects as examples. Errors are shown for non-corrected, AMUSE-corrected and INFOMAX-corrected signals. Due to the frequency content of metallic artifacts, errors are expected to be lower in the alpha band and higher in the delta band, focusing especially on the areas where the artifact is located. Note that AMUSE-based reconstruction shows the lowest errors for the three measures.

Table 1.1: Error percentage for nMSE, delta power and alpha power (average of all channels) for non-corrected signals, AMUSE-corrected signals and INFOMAX-corrected signals.

Subj.	nMSE			Delta error (%)			Alpha Error (%)		
	Non-corrected	Amuse	Infomax	Non-corrected	Amuse	Infomax	Non-corrected	Amuse	Infomax
1	521.70	0.12	414.10	2464.23	0.52	2226.07	2.12	0.31	3.99
2	7811.33	0.33	173.02	44500.04	0.42	214.46	1.30	0.88	121.7
3	43.94	0.02	48.02	84.01	0.15	83.93	0.02	0.07	2.15
4	20926.17	1.51	3622.56	64421.30	2.50	12293.77	0.97	2.52	475.44
5	219.99	0.02	19.68	1568.38	0.13	131.80	0.01	0.06	2.06
6	3754.65	0.21	50.55	14169.41	0.48	66.97	32.76	0.62	42.49
7	9061.74	0.57	3417.17	59869.96	0.80	9964.57	0.01	0.44	1665.48
8	8379.42	0.19	135.58	43106.98	0.22	174.84	0.01	0.12	114.64
9	3795.21	0.13	45.05	14018.33	0.64	39.15	121.08	0.52	38.35
10	3764.70	0.59	205.70	14720.35	1.33	308.99	148.16	2.01	102.39
Mean	<b>5827.89</b>	<b>0.37</b>	<b>813.14</b>	<b>25892.30</b>	<b>0.72</b>	<b>2550.45</b>	<b>30.64</b>	<b>0.75</b>	<b>256.87</b>

### 1.3.4 Real data

Once the effectiveness of the automatic BSS-based procedure has been measured using simulated signals, assessment of its performance with real MEG data is pertinent. Real spontaneous MEG signals with eyes closed corresponding to the 10 subjects with ferromagnetic implants described in the 'Materials and Methods' section were used for this purpose. One way to demonstrate

the filtering performance is to show that alpha-band oscillations with eyes closed can be better detected after artifact removal.

Figure 1.7(a) shows as an example a five-second epoch corresponding to a subject with a metallic subdural grid affecting the posterior region of the scalp where a high interference is clearly noticeable. The AMUSE algorithm, which has been shown to be the most effective and efficient technique in the simulated database, was used for the BSS decomposition. After applying the filtering procedure (see figure fig:1-7(b)), alpha waves could be easily recognized by visual inspection. Moreover, topographic maps of the average alpha power of the 10 subjects with metallic implants before and after applying the automatic procedure are shown in figure fig:1-8. Although metallic artifacts mainly affected the delta and theta bands, the alpha-band is also significantly affected, as shown in figure fig:1-8(a) where alpha power is scattered over the scalp due to metallic interference. Once the BSS-based artifact reduction procedure was applied, the map shows a physiologically more plausible distribution of alpha power mainly focused on the posterior region, as expected.

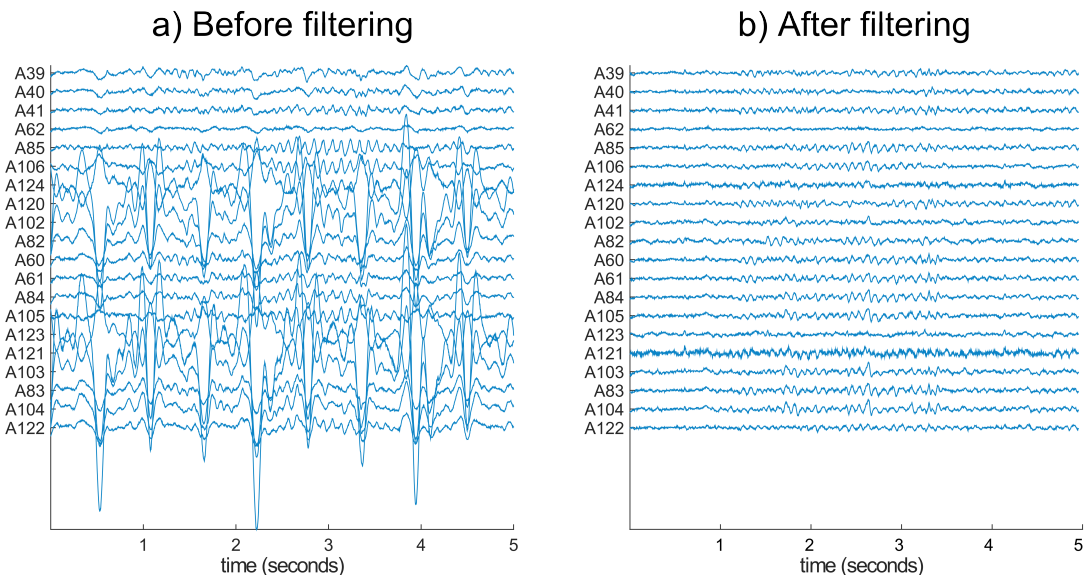


Figure 1.7: (a) Five-second epoch of raw MEG signals containing prominent metallic interference. Posterior channels are shown as an example. (b) Corrected MEG signals obtained after applying automatic AMUSE-based metallic removal procedure.

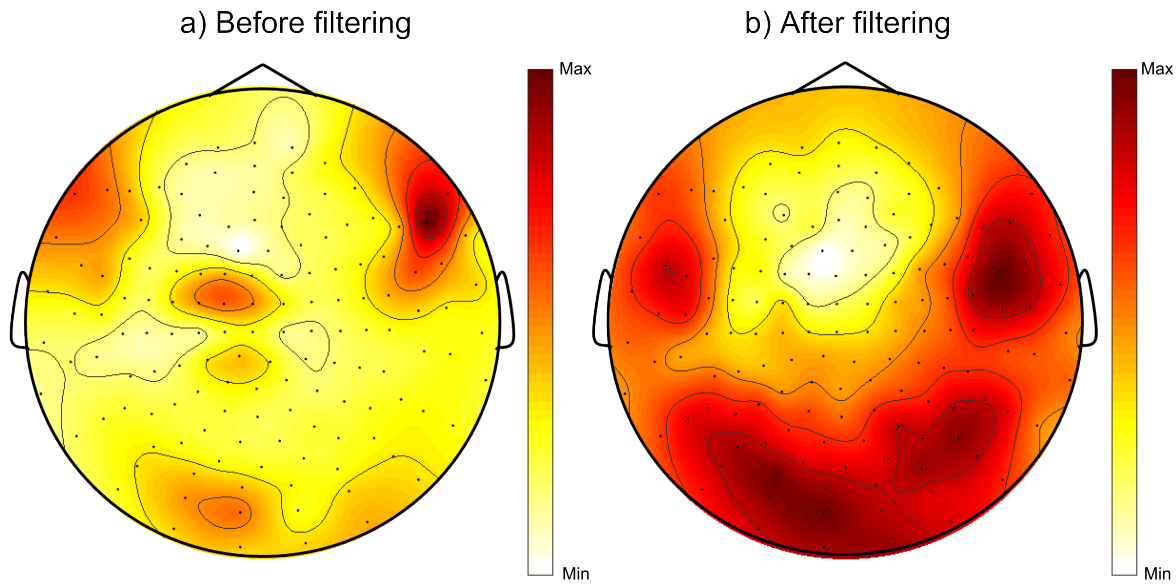


Figure 1.8: (a) Topographic distribution of the average alpha power of the 10 artifactual subjects. (b) Average of alpha power obtained after applying automatic AMUSE-based metallic removal procedure.

## 1.4 Discussion

Metallic artifacts in MEG recordings are an important issue in the diagnosis of neurobiological events because they can hugely distort MEG signals and render many single-channel signals unusable. This leads to an unavoidable loss of information regarding the activity of the brain, or even worse, to a rejection of the MEG technique as a mean to obtain reliable cerebral signals of those patients who have metallic elements that could generate such interferences.

Signal space separation (SSS) (?) and temporal SSS (tSSS) (?) are also methods for MEG filtering. Applying SSS or tSSS is highly advised for Elekta-Neuromag systems (?) and their algorithms are provided by a software registered and available only on this equipment. On the other hand, the filtering approach presented in this paper is based on BSS standard libraries which are freely available and could be used with signals from different MEG systems such as CTF/VSM, 4D Neuroimaging, Elekta and Yokogawa.

The tSSS algorithm was applied efficiently to remove MEG artifacts in several studies (???) and in particular, in the case of metallic interferences: (???). These studies showed the improvement of dipole fitting procedures when tSSS is applied instead of SSS but they did not evaluate the

noise reduction of metallic interference or measure it quantitatively. Furthermore, there are no comparative studies of this technique with other artifact reduction algorithms such as BSS or epoch rejection.

In (?) an interesting SNR analysis was carried out when SSS and tSSS were first applied followed by the BSS or epoch-rejection procedure. This study concluded that SNR increased by 100% after applying SSS or tSSS techniques. Moreover, the SNR improved an additional 33–36% when BSS methods were subsequently applied. The latter suggests that not all noise was successfully removed by the tSSS method and BSS algorithms could remove interferences that remained after applying tSSS techniques. In addition, these studies also concluded that one of the main drawbacks of BSS-based noise-reduction techniques is the need for manual selection of noisy or artifactual components, which is done visually. However, our study describes an automatic approach to detect artifactual components.

As the location and intensity of metallic artifacts usually varies among different subjects, it is not possible to make feasible *a priori* assumptions on these characteristics to adjust an automatic detection algorithm. In this work, a new BSS-based automatic procedure using freely available standard libraries was presented to identify components related to metallic activity, whose performance was tested using simulated MEG signals, which are essential to objectively quantify the effectiveness of the method while reproducing standard clinical situations as faithfully as possible.

One of the main questions arising when working with BSS is the estimation of the number of independent components (ICs) to be extracted. At most, it is possible to extract as many ICs as there are channels that the record is composed of, but when this number is high it is usually advisable to reduce it and usually a lower number of ICs is obtained. The search for the optimal number allows one to avoid over- and under-fitting phenomena (?), and is often achieved by selecting the ICs that can explain a high percentage of the variance of the signals. Due to the high amount of energy accounted for by metallic artifacts, the reduction of the number of ICs was not appropriate when dealing with this kind of interference. The energy of the artifacts was much greater than that of cerebral signals (around four orders of magnitude in some cases) and consequently the number of ICs corresponding to very high percentages of the total variance

resulted in being very low. Thus, it was not possible to achieve a successful separation between cerebral activity and metallic interferences. For this reason, all BSS algorithms were forced to extract as many components as available channels.

One Second-Order Statistics (SOS) and two Higher-Order Statistics (HOS) techniques were tested. The SOS-based algorithm, AMUSE, showed considerably lower errors and therefore a valid decomposition. In the case of HOS, two algorithms were tested, INFOMAX and FastICA. While the first one was successful in separating ICs related to brain activity from those of metallic interference, the second did not manage to generate a valid decomposition. FastICA is an algorithm that uses the kurtosis to evaluate the gaussianity in order to separate independent components. This algorithm is very effective in dealing with supergaussian sources such as cardiac and ocular interferences (kurtosis higher than 3), but its principal drawback is poor convergence when working with gaussian and subgaussian signals, which is the case for metallic interferences that, in general, present a kurtosis value close to 3. Even after ensuring convergence by means of the stabilizer provided by (?), the decomposition was not effective and no metallic-related components could be identified.

On the other hand, the extended version of INFOMAX was able to work with subgaussian signals, and effective convergence and IC separation were achieved. However, the algorithm was not able to separate metallic components as accurately as AMUSE, and part of the cerebral signals remained, mixed with metallic components. That is the main reason why some of the error measures increased significantly when INFOMAX was applied.

After source decomposition, a simple two-step procedure for metallic-related component identification was applied. This simple scheme, based on two criteria which exploited the basic characteristics of metallic artifacts (low frequency and regularity), allowed the delimitation of an artifactual region. Once this region was obtained, all possible ICs that exhibited artifactual behavior were identified and removed from the reconstruction matrix.

This artifact-filtering methodology was tested on 10 sets of simulated MEG signals consisting of clean recordings to which metallic artifacts were added. The extraction of these artifacts from real signals was performed taking into account the different morphologies and varying propagation of this contamination by means of filtering, correlation and estimation of propagation

coefficients by linear regression.

Results showed that the two-step automatic detection methodology was able to detect ICs related to metallic interference especially when they were extracted through the AMUSE algorithm. Normalized MSE error showed an average value of 0.37% (see table 1.1). Errors in delta power were lower than 1% in average, showing a great performance in the most affected spectral band.

It is notable that these error measures presented very low values when compared to non-corrected sets of signals. However, there were some cases in which alpha power showed a slightly higher error (worst case subject 4, 1.55% in excess) but this amount can be considered negligible with respect to the general improvement achieved.

Moreover, the performance of the automatic BSS reduction method was assessed in real MEG signals. Results showed that even high-amplitude metallic interference was properly removed from the MEG data. A study based on the alpha activity confirmed that the BSS-based procedure was able to reduce the metallic artifacts and show a more plausible topographic distribution of alpha-band signal after filtering.

Therefore, after applying the fully automated BSS procedure in simulated and real artifactual MEG data, it can be concluded that AMUSE is the most suitable technique to be used along with the two-step algorithm presented in this study for effectively removing metallic interference from MEG signals.

## 1.5 Acknowledgments

CIBER-BBN is an initiative of the Instituto de Salud Carlos III, Spain. This work has been partially supported by the Ministry of Economy and Competitiveness (MINECO), Spain, under contracts DPI2011-22680 and DPI2014-59049-R and the Ministry of Education, Culture and Sports (MECO) FPU12/05631.

# Notes

- You have to change this running title . . . . . 2